Maximizing Value from available data via Advanced Geostatistical Inversion in the Growler Field

Alessandro Mannini
Beach Energy Limited
Alessandro.Mannini@beachenergy.com.au

Diogo Soares Cunha
Beach Energy Limited
Diogo.Cunha@beachenergy.com.au

Jimmy Ting
GeoSoftware Sdn Bhd
Jimmy.Ting@geosoftware.com

SUMMARY

The Growler field produces oil from the middle Birkhead formation. The main production area is a low relief four-way dip closure consisting of channel reservoir with thickness of ~15-20m that has been mapped from the 3D seismic amplitudes and confirmed by wells. Interpretation of the thin and lower quality oil reservoirs in the form of secondary channel and floodplain sandstone deposits from the seismic has not been successful. The inability to discriminate and delineate the geological and/or fluid facies is the main challenge to further explore and develop the field. The challenge is worsened by the uncertainty in the well logs and the poor-quality nature of land seismic data.

An advanced pre-stack geostatistical inversion study has been carried out aiming to solve the observed key issues: i) discrimination of different reservoir facies from elastic properties derived from 3D seismic amplitudes; ii) enhancement of the quality of the seismic to resolve the inherent uncertainty associated with the AVO responses; iii) mitigation of the ambiguity of false AVO anomaly due to carbonaceous shale that had led to unsuccessful drilled well.

The applied geostatistical inversion study workflow includes iterative seismic petrophysics and rock physics modeling to produce a good quality and consistent set of well logs; robust seismic data conditioning for removal of coherent and incoherent noises, and alignment of seismic events, with the resultant seismic AVO response calibrated with well data; deterministic inversion of conditioned multiple angle stacks and litho-facies estimation using Bayesian inference to provide understanding on the intricacies of the aforesaid challenges before application of geostatistical inversion. Joint facies and elastic properties inversion facilitated by Bayesian-based geostatistical inversion using Multigrid Markov Chain Monte Carlo algorithm has resulted in highly detailed subsurface facies models that show excellent match at most of the 14 blind wells not used in the study.

Key words: Channel reservoir, floodplain sandstone, geostatistical inversion, AVO, iterative seismic petrophysics and rock physics modeling, Bayesian inference.

INTRODUCTION

The Growler field located in the Cooper–Eromanga Basin, South Australia, is an onshore field producing oil from the middle Birkhead formation of Jurassic age. Figure 1 shows the location of the Growler field and the stratigraphy and lithology of the Eromanga Basin. The main producing area under the current study is a low relief four-way dip closed structure consisting of a channel reservoir of 15-20m thickness that has been mapped from the 3D seismic amplitudes and confirmed by the drilled wells. Interpretation of 3D seismic data has revealed relatively lower quality oil reservoir in the form of minor sandstone channel, crevasse-splay, and floodplain deposits to the north of the main structure. To draw strategy for optimum development of this field as well to support further exploration campaign pre-stack seismic inversion has been carried out.

The objective of the study is to derive a highly detailed subsurface facies models solving several challenging problems in this area. Some of the key issues to solve are: i) discrimination of different reservoir facies from elastic properties derived from deterministic inversion due to their substantial overlap, ii) inherent uncertainty associated with the AVO (Amplitude Versus Offset) responses due to poor quality of land seismic data requiring optimal preconditioning of the seismic gather data; and iii) mitigation of the ambiguity of false AVO anomaly due to carbonaceous shale that had led to unsuccessful drilled well.

An innovative workflow comprising iterative seismic petrophysics and rock physics modeling, preconditioning of seismic data for removal of both coherent and incoherent noise and seismic event alignment was used to calibrate the seismic AVO response with well data. Deterministic inversion of multiple angle stacks was carried out and litho-facies estimated using Bayesian inference to understand the intricacies of the aforesaid challenges before application of geostatistical inversion to derive highly detailed subsurface model. Joint facies and elastic properties inversion facilitated by geostatistical inversion using Multigrid Markov Chain Monte Carlo method has resulted in good quality facies results that match wells at several blind locations and conform to the depositional setup of the area.

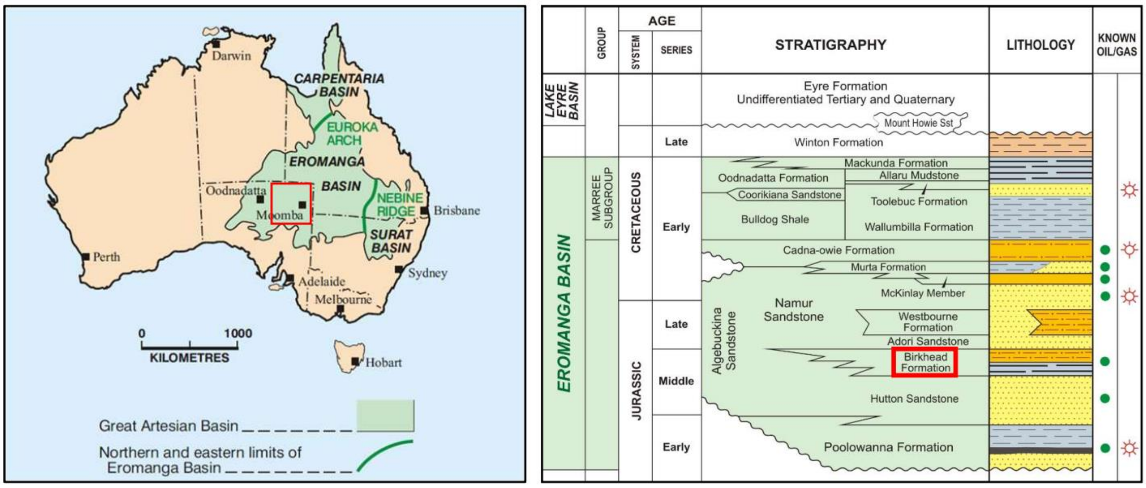

Figure 1. Left: The red box indicates the location of the Growler field; Right: The general stratigraphy and lithology of the Eromanga Basin highlighted with the Middle Jurassic Birkhead Formation containing known oil reservoirs.

STUDY WORKFLOW

Different elements of the workflow used in the present study comprises i) seismic data conditioning, ii) integrated and iterative well log conditioning, seismic petrophysical evaluation and rock physics modeling, iii) deterministic inversion and iv) geostatistical inversion. The work elements have been used iteratively rather than in sequential fashion to achieve the objectives of this study.

Seismic Data Conditioning and Enhancement

The seismic data used in the study is of reasonable quality for the time window of interest. The Birkhead formation has relatively weaker seismic amplitude and lower signal-to-noise compared with the overburden. Class III type AVO response expected in the oil-bearing zone is quite subtle in the current seismic data. Besides, anomalously strong amplitudes in angle stacks up to 15 degrees has apparently distorted the AVO gradient. Seismic conditioning workflow has been designed to remove remnant multiples, random and coherent noise to improve the AVO information. One pass of radon-demultiple and three passes of random de-noise processes were applied starting from the gather data which has NMO (Normal Moveout) with Eta (η) correction and trim statics already applied. Figure 2 shows the comparison of the seismic data before and after conditioning. As it could be seen, the anomalously high amplitude of the near stack has been attenuated while the far stack shows improved seismic continuity and details after conditioning. The effect of seismic data conditioning was assessed at selected well locations using seismic-well ties as well as a first pass deterministic AVA (Amplitude Versus Angle) simultaneous inversion to ascertain if the desired level of noise removal was achieved without deteriorating the seismic signal. A section of inverted P-Impedance and Vp/Vs (Figure 3) clearly shows that conditioned data yields more consistent and reasonable elastic properties variation for the Birkhead formation, apart from the improved match at the well locations. The shale with high Vp/Vs at GC40 as well as GC34 sand packages have been resolved much better compared with the inverted results derived from the angle stacks before seismic data conditioning.

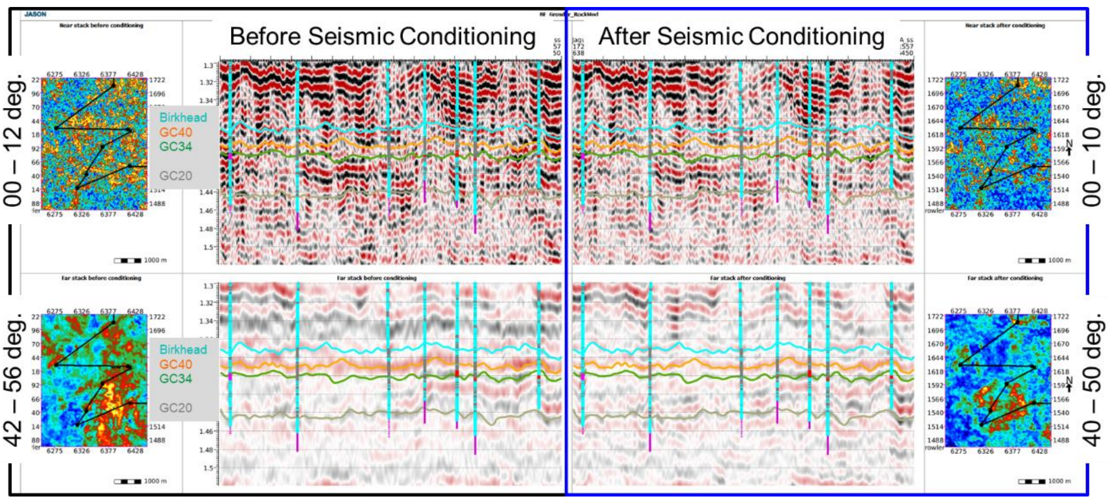

Figure 2. Near and far angle stacks before (left) and after (right) seismic data conditioning. The adjoining maps show corresponding root mean squares attributes. The conditioning process has attenuated the strong amplitude of the near stack while the far stack shows improved seismic continuity after conditioning.

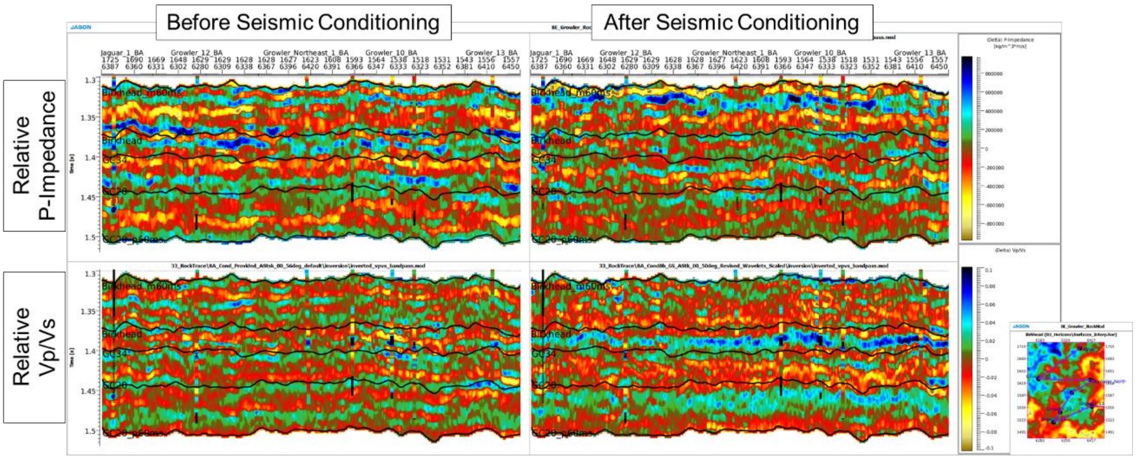

Figure 3. Deterministic inversion using seismic data before (left) and after conditioning (right) exhibits significant improvement of match at the well locations. Besides, inversion of conditioned seismic data results in more consistent and reasonable elastic properties variation in the Birkhead formation. The inset shows the Birkhead horizon with outline of the seismic section.

Well Log Conditioning, Seismic Petrophysics, Rock Physics Modeling and Validation with Seismic

Integrated and iterative well log conditioning, seismic petrophysical evaluation, rock physics modeling workflow validated through well to seismic tie and AVO/AVA modeling (Talib et al., 2020) as shown in Figure 4 has been adopted to produce a consistent set of petrophysical and elastic property curves that facilitates a full understanding on the relationship between geology (Facies), petrophysical properties (Volume of Clay, Porosity, and Saturation), elastic properties (P-velocity, S-velocity, and Density), seismic amplitudes, and AVO.

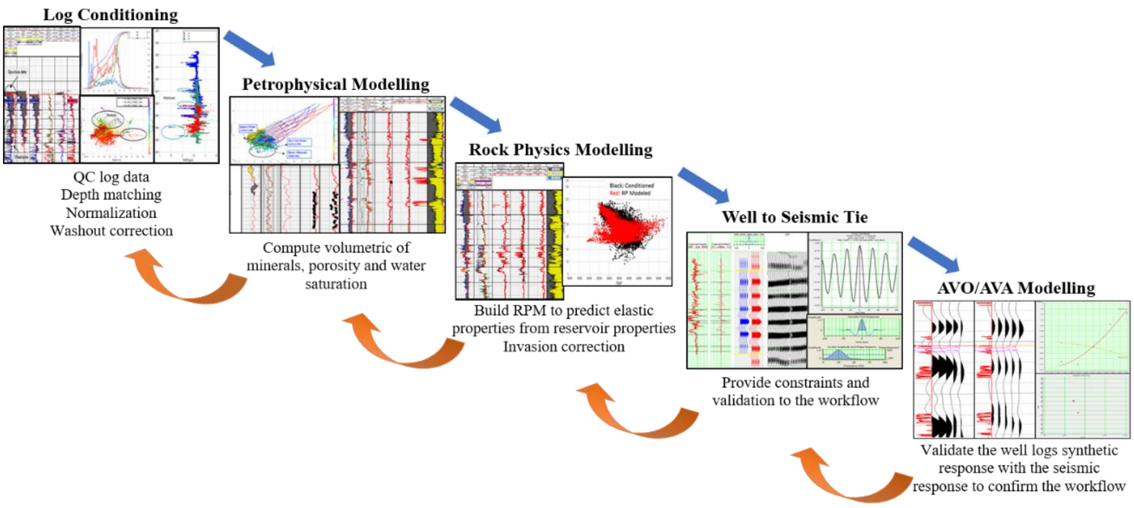

Figure 4. Integrated and iterative well log conditioning, seismic petrophysical evaluation, rock physics modeling workflow validated through well to seismic tie and AVO/AVA modeling (Talib et al., 2020).

Figure 5 shows the crossplot of P-impedance versus Vp/Vs color-coded by Facies, comparing the measured data versus the final rock physics modeled data. The final rock physics modeled logs show consistent trend of elastic properties and significant improvement in facies classification and discrimination. These results have been further validated with seismic data via deterministic inversion as shown earlier in Figure 3.

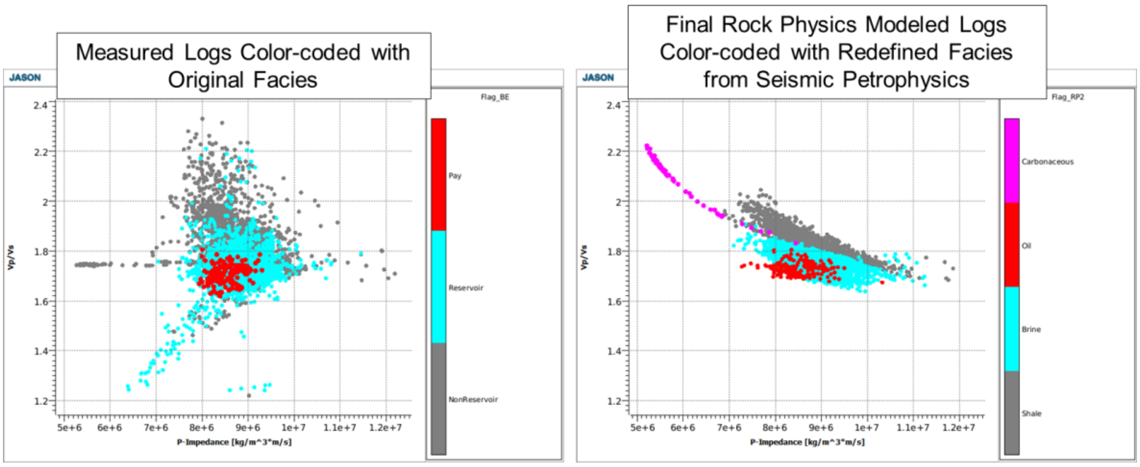

Figure 5. P-impedance versus Vp/Vs crossplots showing significantly improved consistency of elastic property data with the facies in the final rock physics modeled logs (Right) compared to the measured logs (Left).

Well Feasibility

At the resolution of seismic data (or deterministic inversion), only three facies, viz. Non-Reservoir, Reservoir, and Carbonaceous Shale could be defined over the zone of interest. The point bar pay sands that accumulated at the core of the Growler field can just be partially separated at seismic resolution based on the well log data (Left crossplot in Figure 6). In the presence of noise in seismic data, if not properly eliminated/attenuated, it might even be difficult to discriminate the point bar pay sands from other facies using deterministically inverted elastic properties as illustrated in the right crossplot of Figure 6.

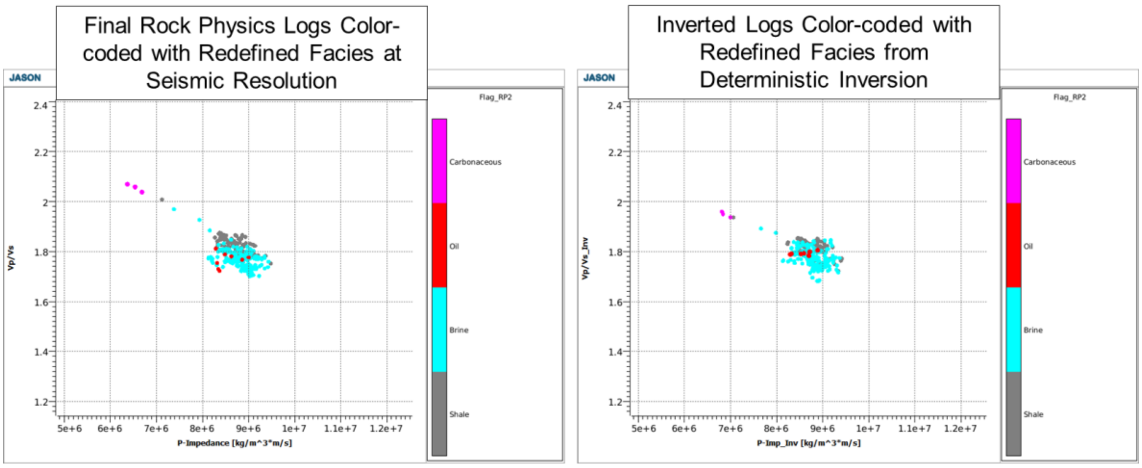

Figure 6. P-impedance versus Vp/Vs crossplots at seismic resolution. Left: Based on the well log data at seismic resolution, Oil sand can just be partially separated; Right: Oil sand might become non discriminable in the inverted pseudo logs extracted from the deterministic inversion probably due to presence of noise in the seismic data.

In order to improve the discrimination and prediction of Facies from the seismic data and exploit the high-resolution capabilities of geostatistical inversion, the Facies logs from the right crossplot of Figure 5 were redefined and classified into 2 levels: Level 1 Facies consisting of Shale, Sand and Carbonaceous Shale; Level 2 Facies consisting of Shale, Cemented Sand, Low Porosity Sand, Medium Porosity Sand, High Porosity Sand and Carbonaceous Shale, as shown in Figure 7. At the geostatistical inversion resolution and with the use of multi-level facies in the geostatistical inversion process, more detailed classification of geologically meaningful facies can be potentially predicted from the seismic data.

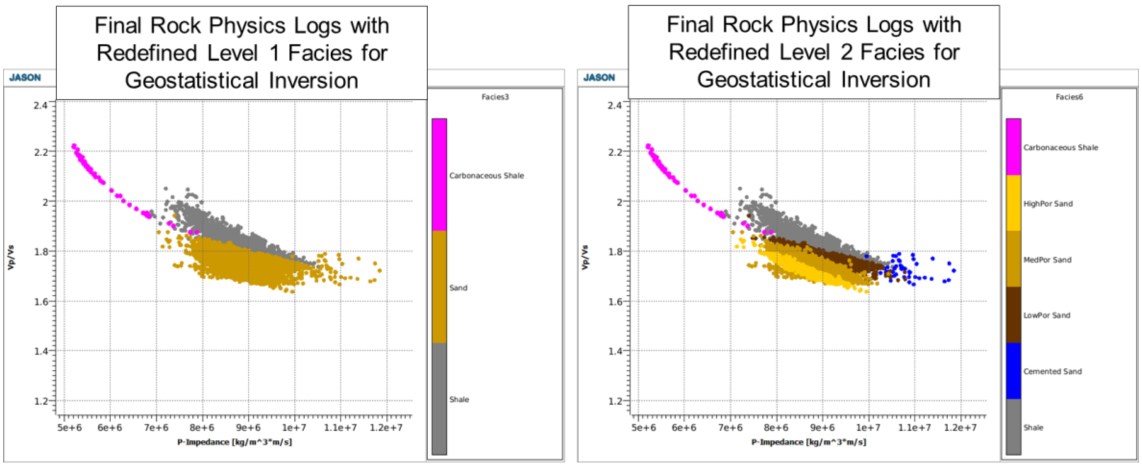

Figure 7. The Facies logs from the right crossplot of Figure 5 are redefined and classified into 2 levels to exploit the high-resolution capabilities of geostatistical inversion: Left: Level 1 Facies consisting of Shale, Sand and Carbonaceous Shale; Right: Level 2 Facies consisting of Shale, Cemented Sand, Low Porosity Sand, Medium Porosity Sand, High Porosity Sand and Carbonaceous Shale.

Deterministic AVA Simultaneous Inversion

Five angle stacks created from the conditioned gather data with angle ranges 0 – 50 degrees have been simultaneous inverted for P-impedance and Vp/Vs. Constrained Sparse Spike Inversion (CSSI) was used in this study (Debeye and van Riel, 1990). In CSSI, the subsurface is represented by minimum number of reflectors and is constrained by the geology of the area to capture vertical trend and lateral continuity of reflections (Contreras et al., 2006). The inversion process is controlled by a set of constraints based on a priori information from the known geology or from well curves. These constraints effectively limit the range of potential solutions to those having geophysical and geological significance. Transformation of seismic reflection traces into acoustic/elastic impedance layer facilitates the recovery of the geologic information contained in the seismic data. Lateral variations in the low frequencies, missing from seismic data, are incorporated via the use of model file derived from final well log data as the trend.

The results of deterministic inversion are interpreted using the principle of Bayesian inferences. The most likely facies and the probability of the reservoir facies are shown in Figure 8. The reservoir is then delineated using geobody checking process based on the reservoir probability of >50% as the cutoff value, as shown in Figure 9. The point bar sand in the producing area is well captured with this method.

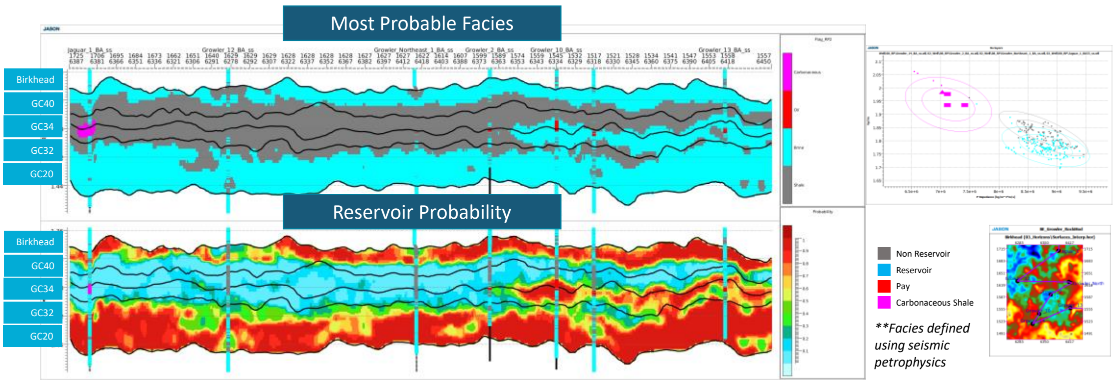

Figure 8. Most probable facies and reservoir probability volumes interpreted from deterministic inversion results using Bayesian inference for three facies, viz. Non-Reservoir, Reservoir, and Carbonaceous Shale. Right top panel shows the 2D probability density functions of P-impedance and Vp/Vs per facies.

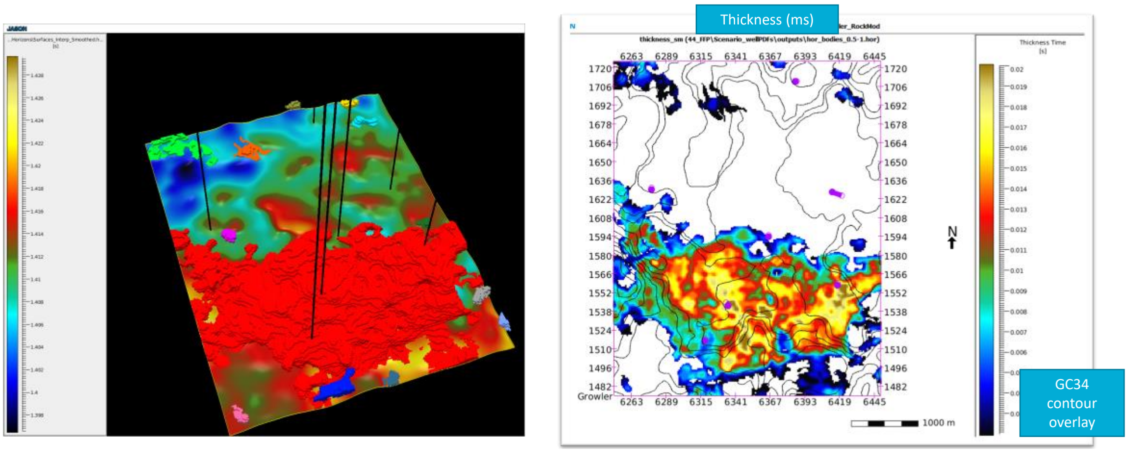

Figure 9. Point bar sand at the core of the Growler field delineated using geobody checking process based on the reservoir probability volume from deterministic inversion with cutoff value above 50%.

Advanced AVA Geostatistical Inversion

Analysis of deterministic inversion results provided with, much deeper insight into the challenges posed by data quality and data inadequacy issues while integrating multidisciplinary data, e.g., well logs, seismic partial angle stacks, structural interpretations, etc. in the previous stages. All these issues are addressed in geostatistical inversion where multiple realizations of litho-facies and elastic properties have been derived jointly to cover various possible scenarios of the subsurface. The results of geostatistical inversion provide with higher level of details beyond resolution of seismic data and deterministic inversion.

Goodman and Sokal (1998) have given a detailed description of Multigrid Markov Chain Monte Carlo algorithm to sample the multi-dimensional and multi-modal posterior probability density function. In geostatistical inversion, the posterior probability density function is obtained by combining the prior knowledge of facies proportion with the likelihood of elastic properties, under Bayesian framework (Contreras et al., 2014). In essence, it is a paradigm of joint inversion where the models of the facies (discrete properties) and elastic properties (continuous properties) evolve simultaneously (Debeye, 2018 and 2019) during the inversion process. Seismic data helps to accept or reject proposals to update the evolving model. To keep the process unbiased, geostatistical inversion is run in two stages. In the first stage, an unconstrained inversion is run where none of the well properties, whether discrete or continuous, are used as hard data. The premise is that the parameters of the geostatistical model selected during modeling should bring out the targeted fine details of the subsurface when seismic data is used along with the appropriate wavelets with seismic signal to noise ratio being a free parameter to vary. If required, geostatistical model is updated till the results of geostatistical inversion show reasonable match with the wells which are kept as blind to this process. Once satisfactory results are obtained, the wells properties, both facies and elastic, are set as constrained wells and inversion is run again - this stage being called the constrained inversion. It is imperative to note that all wells with good quality data, which provide valuable prior information for geostatistical inversion should be used as constraints. A total of 81 highly detailed realizations of equi-plausible reservoir descriptions were generated to derive statistically stable results and also capture the uncertainty due to bias comprising the uncertainties in facies proportions, vertical and lateral variogram ranges, seismic noise, etc.

Figure 10 shows the comparison between the sand probabilities generated from deterministic inversion results and the sand frequency generated from the 81 realizations of geostatistical inversion results. Geostatistical inversion shows improved sand prediction with higher resolution yet honoring seismic amplitudes. Additional sands are predicted in the north-west and north-east side of the core of Growler field, which was not predicted by deterministic inversion. These sands are floodplain deposits with much lower Net-to-Gross ratio.

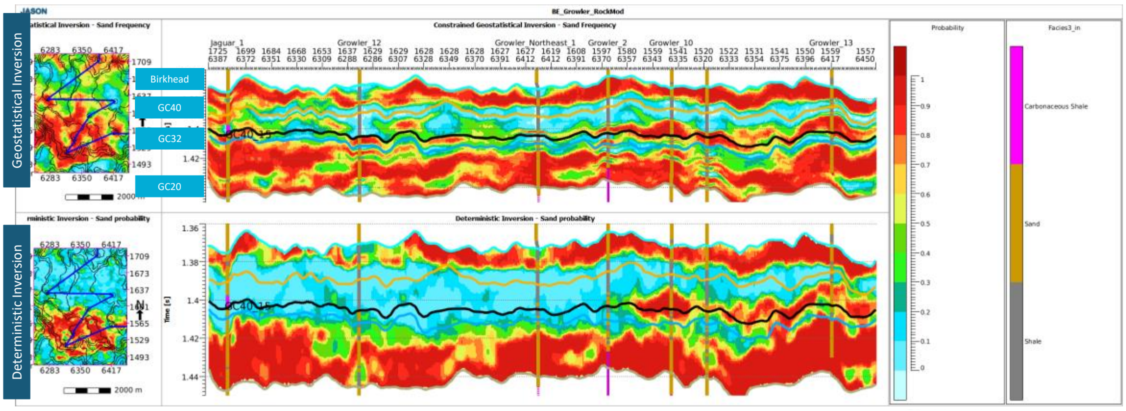

Figure 10. Better sand prediction with improved resolution attained with geostatistical inversion results (top) compared with deterministic inversion results (bottom). The black line in the cross-section indicates the stratigraphic slice position currently displayed in the maps. Note the additional sand prediction to the north of the main producing field from the geostatistical inversion, which is mostly related to the floodplain deposition.

At the end of the geostatistical inversion process, drilling results at 14 blind wells (not used till now) were investigated to assess the accuracy of the study results. Thickness of sands in the reservoir interval was computed from the reservoir sand flags for each of the wells and compared with those derived from geostatistical inversion. Predicted sands thickness from the 81 realizations of geostatistical inversion results at each of the blind well location were calculated and ranked as cumulative normal distribution function (CDF) (Left picture in Figure 11). To assess the accuracy of prediction, the measured sand thickness at each of the 14 blind wells was used to find out the value on the CDF. Measured sand thickness falling within the range P30-P50 is considered good, within P10-P30 or P70-P90 is considered moderate and below P10 or above P90 is considered as a poor prediction. The results of this analysis as shown in the two tables on the right side of Figure 11, have shown that the actual reservoir sand thickness for all the wells except for one of the horizontal wells are well predicted within the P10 and P90 range; 57% of the wells show good match; and 36% of the wells show moderate match.

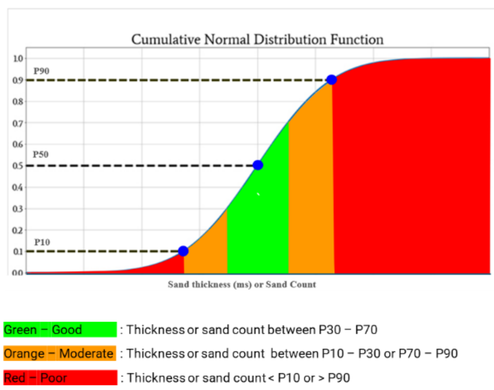

Vertical Wells	Reservoir Sand Thickness (ms) at the well	Sand Thickness (ms) Calculated from Ranking Process		
		P10	P50	P90
Growler_1	10	7	11	14
Growler_3	12	8	10	13
Growler_4	11	5	8	11
Growler_5	10	4	8	13
Growler_6	11	8	11	14
Growler_7	12	9	12	15
Growler_8	13	8	10	14
Growler_9	10	6	9	13
Growler_11	11	6	10	12
Horizontal Wells	**No. of ResFlag Sample at the well**	**No. of Sand Sample from Ranking Process**		
		P10	P50	P90
Growler_15	21	8	13	18
Growler_16	51	14	35	53
Growler_17	40	32	37	44
Growler_18	34	26	35	44
Growler_NE2	51	34	50	66

Figure 11. Blind well analysis using quantitative approach via ranking: Reservoir sand thickness (vertical wells) or reservoir sand count (horizontal wells) are compared with the cumulative distribution function at the respective well location for the probability. Note that the blind wells sand thickness/count are well predicted within the P10 and P90 range.

CONCLUSIONS

A careful well data guided seismic conditioning, together with the seismically validated, integrated and iterative well log conditioning, seismic petrophysical evaluation and rock physics modeling approach was successfully used for detailed reservoir characterization study in the Growler field. Use of geostatistical inversion has tightly integrated the conditioned seismic data and rock physics modeled logs to extract highly detailed reservoir model from the seismic data. The accuracy of the results of this study have been assessed quantitatively by extensive blind well analysis. Sand encountered in most of the blind wells were found to lie between P10 to P90 giving rise to high level of confidence to use these results for future field optimization and development.

ACKNOWLEDGMENTS

The authors would like to express their gratitude to the Management of Beach Energy Limited for the permission to publish this paper. They also thank colleagues from Beach and GeoSoftware for their technical contribution in this study.

REFERENCES

Contreras, A., C. Torres-Verdin and T. Fasnacht, 2006, AVA simultaneous inversion of partially stacked seismic amplitude data for spatial delineation of lithology and fluid units of deepwater hydrocarbon reservoirs in the central Gulf of Mexico: Geophysics, 71, p. E41-E48.

Contreras, A., C. Torres-Verdin, T. Fasnacht, W. Chesters and K. Kvien, 2014, Joint stochastic inversion of 3D prestack seismic-amplitude data and well logs for high-resolution reservoir characterization of deepwater hydrocarbon reservoirs, The Leading Edge, 33, May, 520-525.

Debeye, H.W.J. and P. van Riel, 1990, Lp-norm Deconvolution: Geophysical Prospecting, Vol. 38, p. 381-403.

Debeye, H.W.J., 2018, Solving for facies in seismic inversion as essential for realistic reservoir models: Expanded Abstracts, 80th EAGE Conference & Exhibition, Copenhagen, Denmark, WS05.

Debeye, H., 2019, Spatial Continuity and Simultaneous Seismic Inversion of Facies and Reservoir Properties Ready for Flow Simulation: Conference Proceedings, Fourth EAGE Conference on Petroleum Geostatistics, Florence, Italy, WePG13.

Goodman, J. and Sokal, A., 1989, Multigrid Monte Carlo method. Conceptual foundations. Physical Review D - Particles, Fields, Gravitation and Cosmology, 40(6), 2035-2071.

Talib, M., M.Z.A. Durrani, A. Mathur, R.P.A. Bekti and J. Ting, 2020, Integrated Petrophysics and Rock Physics Workflow Validated by Well to Seismic Tie and AVO Modelling: Expanded Abstracts, Fifth EAGE Workshop on Rock Physics, Milan, Italy, RP06.